Estuarine, Coastal and Shelf Science 315 (2025) 109177

Contents lists available at ScienceDirect

Estuarine, Coastal and Shelf Science

journal homepage: www.elsevier.com/locate/ecss

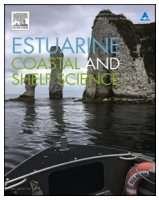

Do vegetated intertidal areas alter currents on an estuarine scale?

Jesse Bootsma [a,*], Bas W. Borsje [a], Daphne van der Wal [b,c], Suzanne J.M.H. Hulscher [a]

[a] Marine and Fluvial Systems, Faculty of Engineering Technology, University of Twente, Enschede, the Netherlands
[b] Water Resources, Faculty of Geo-Information Science and Earth Observation, University of Twente, Enschede, the Netherlands
[c] Department of Estuarine and Delta Systems, NIOZ Royal Netherlands Institute for Sea Research, Yerseke, the Netherlands

ARTICLE INFO

Keywords:
Saltmarsh species
Currents
Decadal timescale
Eco-hydrodynamic modelling
Spatially extended effects
Scheldt estuary

ABSTRACT

Intertidal areas often host tidal marsh vegetation, which plays a crucial role in influencing hydrodynamic processes. This study investigates the influence of saltmarsh vegetation on fringing and mid-channel flats on currents in the Western Scheldt, the Netherlands. We quantify how and over which spatial scale vegetated intertidal areas affect estuarine currents, and how this varies over time when vegetation cover changes. Using vegetation maps spanning ca 25 years, we assessed changes in saltmarsh vegetation extent and distribution, with notable vegetation expansion on mid-channel flats. A depth-averaged Delft3D-FM model was adopted to quantify the effect of both mono-specific and multi-species vegetation on peak ebb and flood currents. Results indicate that species diversity is particularly important when considering currents at the marsh-mudflat scale, and its effect is negligible at the broader estuarine scale. During storm conditions, mono-specific and multi-species vegetation reduced peak velocities by 10–80% on the vegetated zone, and by 1–30% in the surroundings, over an area comparable to or smaller than the vegetated zone. During calm-weather conditions, the effect was limited to the vegetated zone (10–80%, although with smaller magnitude and extent compared to storm conditions). Over the period 1993–2016, both bathymetrical changes and changes in vegetation had a comparable magnitude of impact on altering current velocities over the saltmarshes. These findings emphasize that saltmarsh vegetation alters currents at the marsh-mudflat scale in particular. This will have estuary-wide implications for sediment dynamics, morphology and ecology over a timescale of decades.

1. Introduction

Estuaries are dynamic environments where fresh water from rivers meets salt seawater, creating complex and variable hydrodynamic conditions. These areas are vital for various economic activities, including port logistics and fishing, and are also valued for their ecological services. Within estuaries, intertidal zones are particularly important due to their role in modulating waves and currents (Bouma et al., 2005a; Möller et al., 2014; Rupprecht et al., 2017; Temmerman et al., 2005; Willemsen et al., 2020). Intertidal areas often host tidal marsh vegetation, which plays a crucial role in influencing hydrodynamic processes. Vegetation in these zones generally causes a reduction in average current velocities, wave energy and dampening of turbulence (Leonard and Croft, 2006; Möller et al., 2014; Nepf, 1999). This reduction in hydrodynamic energy promotes increased sediment accretion due to a reduction in bed shear stresses (Shi et al., 2012). Next to the reduction of wave and current energy, vegetated intertidal areas offer additional ecosystem services, including habitat provision (Barbier et al., 2011), erosion control through plant cover, encompassing both aboveground and belowground biomass (Brooks et al., 2021; Cahoon et al., 2021; Shi et al., 2012; Silliman et al., 2019), and carbon sequestration (McLeod et al., 2011).

These ecosystem services highlight the role of saltmarsh vegetation as ecosystem engineering species, as they modify their environment, influence physical conditions, and thereby impact other species (Jones et al., 1994). Understanding how saltmarsh vegetation impacts hydrodynamic conditions is crucial, especially in the context of changing environmental factors such as sea level rise, variations in river discharge, storm surges and sediment supply. Both natural fluctuations and human activities contribute to these changes, which have led to a decline in the global extent of salt marshes over the past few decades (Campbell et al., 2022). Ongoing efforts are taking place to restore intertidal areas, often from a nature-based solutions (NBS) perspective. Marshes in front of dikes, also referred to as vegetated foreshores, receive increasing attention as integrated features in flood safety (Borsje et al., 2011; Bouma et al., 2014; Marin-Diaz et al., 2023; Morris et al.,

* Corresponding author.
E-mail address: jesse.bootsma@utwente.nl (J. Bootsma).

https://doi.org/10.1016/j.ecss.2025.109177
Received 18 November 2024; Received in revised form 29 January 2025; Accepted 31 January 2025
Available online 31 January 2025

2018; Narayan et al., 2016; Sutton-Grier et al., 2015; Temmerman et al., 2013, 2023; van Zelst et al., 2021; Vuik et al., 2016). Changes in extent, morphology and vegetation cover alter the impact these systems have on hydrodynamics (Bouma et al., 2005b; Koch et al., 2009; Maza et al., 2015; Stark et al., 2017a; van Veelen et al., 2020; Willemsen et al., 2020; Ysebaert et al., 2011). To integrate vegetated intertidal areas in NBS's, we need to understand the interaction between vegetation dynamics and ecosystem engineering capacity, both at local levels and through spatially extended effects. The biomechanical characteristics of vegetation species influence their impact on currents and waves, which can be used as a proxy for ecosystem engineering capacity (Bouma et al., 2005b). While much of the existing research has focused on the impact of vegetation on waves, understanding its effects on currents is equally important. Key morphological traits, such as vegetation height, stem diameter and stem flexibility, play a significant role in this interaction. Environmental changes can cause shifts in vegetation species and therefore modify the impact on currents (Crain et al., 2004; Zhu et al., 2020). Within estuaries, salinity and inundation frequency largely define ecosystem habitats (Crain et al., 2004; Guerra-Chanis et al., 2022; Neubauer, 2013; Pennings et al., 2005). Therefore, when moving from the saltwater region near the mouth towards the brackish and freshwater regions further upstream, these habitats change, thereby impacting the distribution of intertidal vegetation (Zhu et al., 2020).

In addition to the biomechanical properties of vegetation, the impact of saltmarsh vegetation on currents and waves also depends on meteorological conditions. During storm conditions, elevated water levels cause a higher submergence rate of the vegetation (the ratio of vegetation height to water depth), generally leading to a reduced impact on hydrodynamic energy (Maza et al., 2015). Nevertheless, for flood safety, these storm conditions are critically important. Calm-weather conditions, which prevail for most of the year, should not be overlooked, as they can play a role in estuarine dynamics (for instance in geomorphological or ecological processes, e.g. (Z. Hu et al., 2018; Willemsen et al., 2020)).

At the plant and marsh scale, the impact of saltmarsh vegetation on currents is thoroughly studied (e.g. Leonard and Luther, 1995; Nepf, 1999; Temmerman et al., 2005). The physical structure of plants modifies the flow through additional drag. This typically results in reduced current velocities, dampening of turbulence and changes in flow routing (Leonard and Croft, 2006; Leonard and Luther, 1995; Nepf, 1999; Temmerman et al., 2005). When water flows onto a marsh, there is usually a sudden increase in turbulent kinetic energy (TKE), and in some cases an increase in current velocity, at the vegetated edge. However, just a few meters into the marsh, TKE and current velocities are drastically reduced (Leonard and Croft, 2006; Leonard and Reed, 2002; Neumeier, 2007; Neumeier and Amos, 2006; Tempest et al., 2015). This reduction in flow velocity can be offset by a negative water level gradient. Subsequently, the delayed drainage of the marsh can create a positive water level gradient, which in turn enhances ebb currents.

In contrast, studies on the scale of an entire estuary are less common, although some studies exist (Bennett et al., 2023; Fairchild et al., 2021; Stark et al., 2017b). Stark et al. (2017b) performed a study on the impact of the elevation of intertidal flats and the location of managed realignment sites on estuarine tidal hydrodynamics in the Scheldt estuary. They found that both their position along the estuary and the ratio of their storage volume to the local tidal prism govern the extent and magnitude of the impact on tidal hydrodynamics. Furthermore, in a study by Bennett et al. (2023), the impact of marsh vegetation on wider estuarine hydrodynamics was explored. Their results show that marsh vegetation is able to reduce tidal amplitudes, both on the marsh platform and proximity, and the wider estuary. Additionally, changes in residual currents were observed on the marsh platform, as well as in tidal channels and saltmarsh creeks. These residual currents, which represent the net flow of water over a tidal cycle after averaging out the effects of oscillating tidal currents, play a crucial role in sediment transport. The three estuaries studied by Bennett et al. (2023) are classified as small estuaries (5.2–45 km^2 respectively), and have an extensive coverage of vegetated intertidal area (200–2200 ha respectively). Therefore, the effects of saltmarsh vegetation on estuarine hydrodynamics in smaller estuaries are expected to be more extensive compared to larger estuaries with smaller ratios of vegetated intertidal area to estuary area.

Although some studies exist on the estuary-scale impact of vegetated intertidal areas on hydrodynamics, these often include a spatially uniform vegetation parametrization (Bennett et al., 2023; Willemsen et al., 2020) by using representative biomechanical vegetation properties i.e. uniform height, stem diameter and stem density. Furthermore, temporal variation in the impact on estuary scale hydrodynamics is understudied since existing studies mainly focus on a single snapshot in time (Bennett et al., 2023). Studies using remote sensing information have indicated, however, that dynamics in estuarine vegetation extent over decades can be significant (e.g., Van der Wal et al. (2008) for the Western Scheldt). At the same time, establishment of vegetation depends on hydrodynamic conditions (e.g. Z. Hu et al., 2015; Wang et al., 2017). To come to an estuary-scale understanding of ecosystem engineering capacity of marsh vegetation, spatially varying vegetation characteristics and multiple years have to be included in the analysis. Therefore, this study aims to quantify the spatial scale over which vegetated intertidal areas affect estuarine hydrodynamics and the temporal variation herein driven by changes in vegetation cover and species composition. To fulfil the aim, three research questions are formulated: 1) How does saltmarsh vegetation in a funnel-shaped estuary change over space on a timescale of decades? 2) What is the impact of spatial variation in vegetation on currents, both in storm and calm-weather conditions? and 3) How have changes in bathymetry and vegetation cover affected the impact on currents? Particular attention is given to the impact of saltmarsh vegetation on currents, as these are the primary drivers of sedimentation and erosion processes. This focus contrasts with previous research, which has predominantly explored the wave-attenuating capacity of saltmarsh vegetation. Furthermore, a comparison across scales is provided to determine whether marsh-mudflat and estuarine scale require a different level of vegetation parametrization.

In this study, the Scheldt estuary on the Dutch-Belgian border is selected as a case study site as a typical funnel-shaped estuary with a full salinity gradient. Reasons for this selection include the availability of data, extensive dynamics in physical processes due to natural and anthropogenic influences, and the presence of spatiotemporal dynamics in vegetation species. The impact of vegetated intertidal areas, both fringing (foreshores) and mid-channel (shoals, bars, flats), is studied using a previously calibrated and validated model in Delft3D-Flexible Mesh (Tiessen et al., 2016). By including different levels of vegetation detail (mono-specific vs multi-species) based on available field data and literature covering ca 30 years, insights into decadal-scale variation of vegetated intertidal areas and their impact on currents are gathered.

2. Methodology

The methods of this paper are divided into two main parts: (1) to study spatiotemporal vegetation dynamics using vegetation maps, which we use in part (2) to model the impact of saltmarsh vegetation on estuarine currents. For the former, readily available vegetation maps of the Scheldt estuary are used. These are the result of regular mapping of vegetation based on aerial false-colour imagery and fieldwork. Based on these maps, changes in total marsh extent, extent per species and species distribution are studied. Subsequently, vegetation is parametrized in the Delft3D Flexible Mesh software (DFM; version 2023.01) within a model schematization of the Scheldt estuary (Tiessen et al., 2016) to study the impact of saltmarsh vegetation on estuarine currents.

2.1. Study area

The estuary under study is the Scheldt estuary on the Dutch-Belgian border (Fig. 1). This paper has a particular focus on the Dutch Western

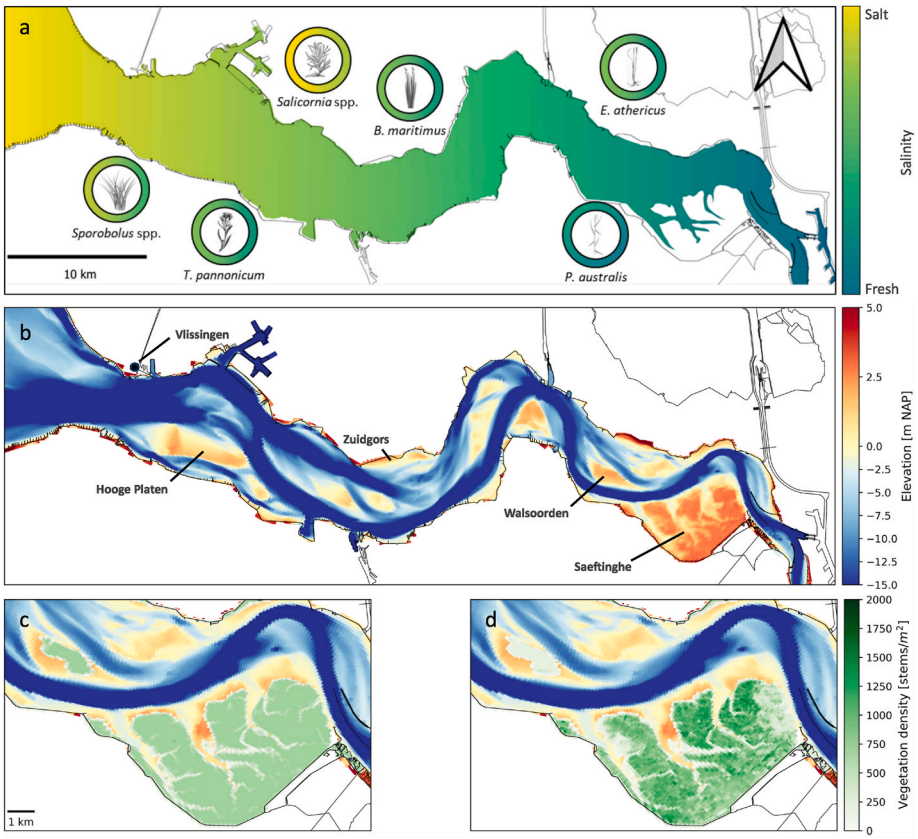

Fig. 1. *The Scheldt estuary on the Dutch-Belgian border with its main saltmarsh vegetation species. A rough estimate of the mean salinity profile is displayed* (Breine et al., 2008)*, showing the salinity range in which each vegetation species is present. (a). The bottom panel presents an overview of the vegetation scenarios (c-d). The 2016 bathymetry (b)* (Tiessen et al., 2016) *and vegetation are shown with a zoom displaying the mono-specific vegetation (c) and multi-species vegetation (d) scenarios, here displayed by the vegetation density. The drawings of Sporobolus* spp.*, B. maritimus and P. australis are from the Integration and Application Network (ian.umces.edu/media-library), licensed under CC BY-SA 4.0. The drawings of T. pannonicum, Salicornia* spp. *and E. athericus are retrieved from Wikimedia Commons (public domain).*

Scheldt, given its significant extent of intertidal area. Tidal influence reaches as far as the sluices of Gent, Belgium, which is 160 km upstream of the mouth near Vlissingen. The estuary is defined as a tide-dominated, meso-to macrotidal estuary, with a tidal range of 3.8 m at the mouth, amplifying to 5.2 m 100 km upstream (near Antwerp), after which it decreases again towards Gent (Meire et al., 2005). Marine waters come from the North Sea at the offshore boundary of the estuary, and river discharge originates from the Scheldt river with a long-term yearly average discharge of ~100 m^3/s (Baeyens et al., 1997). The Western Scheldt is characterized by a multi-channel system of ebb and flood channels, separated by intertidal flats. This multi-channel system reduces to a single channel system near the Dutch-Belgian border. The intertidal flats, both mid-channel and fringing the dikes along the estuary, are home to saltmarsh vegetation species. Currently, the intertidal area covers ~9000 ha, which is much smaller than it was decades ago. Numerous embankments of intertidal area led to a decrease of the estuary area (at MSL) of ~33% between 1650 and 1968 (Van der Spek, 1997). The Braakman is a particular example: this area used to be a tidal inlet but successive empoldering led to a large decrease in area, and in 1952 the tidal arm was completely closed off. Next to the embankments of intertidal area, the navigation channels have undergone repeated deepening and dredging efforts since the 1970s. The channels have been deepened three times, the last of which occurred between 2008 and 2011. During the first deepening, the sediment was largely removed from the estuary, while during the following deepenings the sediment was redistributed over the estuary (Stark et al., 2020 and references therein). While the estuary area of the Scheldt decreased significantly, the tidal prism only decreased by ca 10%, thereby resulting in an increase in tidal range (Van der Spek, 1997). In recent years, efforts have been made to restore and conserve intertidal areas in the Scheldt estuary. Projects such as the "Sigma Plan" in Belgium and the "Natuurpakket Westerschelde" in the Netherlands aim to enhance flood protection and restore natural habitats, respectively.

2.2. Vegetation dynamics

Spatial and temporal changes in saltmarsh vegetation are studied using vegetation maps from Rijkswaterstaat (the Dutch water authority) for the Western Scheldt. These maps are available for the years 1993, 1998, 2004, 2010 and 2016. The 1993 vegetation map does not include the Sieperdaschor, breached in 1990, situated east of the Saeftinghe marsh. Therefore, a separate vegetation map of this marsh from the year 1995 was added to the 1993 vegetation map to ensure similar spatial domain coverage for all years, allowing temporal analysis of the entire domain. The maps were based on false colour aerial photographs to obtain polygons of similar colour, texture, structure and relative height. Subsequently, vegetation communities with key species were assigned to each polygon through fieldwork.

In the current study, information on six vegetation species was extracted from the vegetation maps, namely: *Salicornia* spp. (both *S. europaea* and *S. procumbens*) (Common Glasswort), *Sporobolus* spp. (both *S. anglica* and *S. alterniflora)* (Common Cordgrass, previously known as *Spartina* spp.), *Bolboschoenus maritimus* (Saltmarsh Bulrush), *Phragmites australis* (Common Reed), *Elymus athericus* (Couch Grass) and *Tripolium pannonicum* (Sea Aster). These species were selected for their: 1) presence and abundance (together, these species account for ca 80% of the marsh vegetation in the Scheldt estuary); 2) representation across different salinity levels: ranging from saltwater species to brackish/

freshwater species; and 3) contrasting biomechanical characteristics. Therefore, a contrasting ecosystem engineering capacity can be expected.

Each polygon in the vegetation maps represents one or more vegetation communities. Thus, there may be multiple vegetation communities containing one of the seven vegetation species considered. In our study, we simplified the vegetation maps by combining all vegetation communities that contain one of the seven species considered as a dominant species (e.g., polygons covered by *Sporobolus* spp. for 60% and *Phragmites* spp. for 40% were classified as having *Sporobolus* spp. as the dominant species). However, for the calculation of the areal extent per species, the cover percentage was multiplied by the area of the polygon.

2.3. Model set up

2.3.1. Model description

A depth-averaged model of the Scheldt estuary, previously set up, calibrated, and validated by Deltares, was used in this study (Tiessen et al., 2016). This so-called Nederlands-Vlaams (NeVla) (i.e. Dutch-Flemish model) was constructed in the Delft3D Flexible Mesh software. The model domain covers the entire tide-influenced part of the Scheldt estuary and an offshore part of the North Sea. Grid resolution ranges from 1 to 4 ha in the estuary mouth (~70 by ~160 m) up to less than 1 ha (~50 by ~150 m to ~80 by ~80 m) in the Western Scheldt and Sea Scheldt. The bed roughness, used as a calibration parameter in the original model, was set to a spatially uniform Manning roughness of 0.023 s $m^{-1/3}$ to isolate the effect of vegetation on currents. In the calibration of the original model, saltmarsh vegetation was not considered, although the Saeftinghe marsh was assigned a higher bed roughness. In Supplementary Materials C the difference in peak ebb and flood velocities between the original model and the model with uniform bed roughness is presented. It can be seen that there was limited impact of the changed bed roughness on the validation locations, while a significant impact was observed on intertidal areas, thereby underlining the importance of this study. The D-Flow module was utilized here, which adopts the unsteady shallow water equations (depth-averaged in this case), resulting in a water level and flow field over the model domain. In the Scheldt estuary, tidal currents increasingly dominate the generation of bed shear stresses as one moves further upstream (Z. Hu et al., 2018). Although waves are relevant in the Scheldt estuary (wind waves near the mouth and ship waves further upstream), we focus on currents in this study. The boundary conditions for the model are based on a 2013 hindcast run, with the offshore boundaries defined by water levels along the boundary parallel to the coast and flow velocities along the boundaries transverse to the coast. These time series were derived from a hindcast run of the larger scale model DSCMv6-Zunov4 (Zijl et al., 2013, 2015). The upstream discharge boundaries consist of time series of measured discharges for all tributaries. A spatially uniform wind field was used, which incorporates the potential wind as defined by the KNMI (the Dutch meteorological institute), based on measurements from station Vlissingen. The forces exerted by the wind are coupled to the flow equations as a shear stress, with a constant drag coefficient of 0.0026 for all wind speeds.

2.3.2. Vegetation parametrization

Flow-vegetation interaction in the model was included using the trachytope module, part of the Delft3D-FM software. This module is based on the Baptist equation (Baptist et al., 2007) and determines the flow resistance in a grid cell based on the biomechanical characteristics of the plant species present. This flow resistance is incorporated into the model as an adapted bed roughness. For submerged vegetation, this roughness predictor by Baptist is expressed as (Eq. (1)):

$$C = \frac{1}{\sqrt{\frac{1}{C_b^2} + \frac{C_d n b_v h_v}{2g}}} + \frac{\sqrt{g}}{\kappa} \ln\left(\frac{h}{h_v}\right) \; if \; h > h_v \tag{1}$$

Where C is the net bed roughness, C_b is the initial bed roughness (i.e. for grain and form roughness), C_d is the bulk drag coefficient [-], n is the plant density [stems/m^2], b_v is the stem diameter [m], h_v is the vegetation height [m], h is the water depth [m], g = 9.81 [m/s^2] is the gravitational acceleration and k = 0.41 [-] is the von-Kármán constant. The second term in the equation goes to zero at the transition from submerged to emerged vegetation. Therefore, in the case of emerged vegetation, the roughness predictor becomes (Eq. (2)):

$$C = \frac{1}{\sqrt{\frac{1}{C_b^2} + \frac{C_d n b_v h}{2g}}} \; if \; h < h_v \tag{2}$$

The total effect of vegetation on flow in each grid cell was computed by taking the weighted average values i.e. taking the fraction of the vegetation species present.

2.3.3. Scenarios

From the 2013 hindcast, a period of calm-weather conditions in May and a period of storm conditions in December were selected. In both cases, the model was run for two spring-neap cycles. The storm in December is known as the Sinterklaasstorm (extratropical cyclone Xavier), with a surge peak of 2.5 m (difference between forecasted astronomical tide and actual measured water level during the storm) coinciding with the rising tide during spring tide and wind speeds (10-min average at 10 m above the surface) peaking around 20 m/s predominantly in northwest direction (Carrion Aretxabala, 2015).

To study the impact of saltmarsh vegetation on currents, multiple vegetation scenarios were defined (Table 1). As a baseline, the model was run without vegetation. Secondly, model runs with mono-specific vegetation were performed by incorporating spatially homogeneous biomechanical characteristics for all locations where vegetation is present. Here, biomechanical characteristics of *Sporobolus* spp. were adopted. Thirdly, multi-species vegetation runs were conducted, with the vegetation species distribution derived from the vegetation maps and assigning the biomechanical characteristics of the key species as presented in Table 2.

All three scenarios are run for a vegetation cover corresponding to the year 2016 for the Western Scheldt. Furthermore, a comparison was made between the snapshot of 2016 (combination of bathymetry and vegetation cover) and a snapshot of 1993. This 1993 snapshot was implemented in the model based on the 1993 (+1995 Sieperdaschor) vegetation maps and the 1996 bathymetry for the Western Scheldt, which was the complete bathymetry closest to the year 1993.

2.3.4. Literature-based vegetation characteristics

For each of the six vegetation species included, biomechanical characteristics were derived from literature. An overview of the characteristics used in the model is provided in Table 2**.** The vegetation heights, stem diameters and stem densities have a direct impact on the

Table 1
Overview of model scenarios. (No) refers to no vegetation, (Mono) to mono-specific vegetation, and (Multi) to multi-species vegetation. (93) refers to 1993, (16) to 2016, (c) to calm-weather conditions, and (s) to storm conditions.

Scenario id	Vegetation	Conditions	Snapshot year
No_93_c	No vegetation	Calm-weather	1993
No_16_c			2016
No_93_s		Storm	1993
No_16_s			2016
Mono_93_c	Mono-specific vegetation	Calm-weather	1993
Mono_16_c			2016
Mono_93_s		Storm	1993
Mono_16_s			2016
Multi_93_c	Multi-species vegetation	Calm-weather	1993
Multi_16_c			2016
Multi_93_s		Storm	1993
Multi_16_s			2016

Table 2
Overview of literature-based vegetation characteristics, used as input for the hydrodynamic model.

Species	Height [m]	Stem diameter [m]	Stem density [stems/m^2]	Source
Salicornia spp.	0.30	0.005	200	(Bouma et al., 2013; Schwarz et al., 2018)
Sporobolus spp.	0.60	0.003	700	(Bouma et al., 2013; Schwarz et al., 2018);
Bolboschoenus maritimus	0.7	0.0075	400	Vuik et al. (2018)
Tripolium pannonicum	0.5	0.005	200	van Veelen et al. (2020)
Elymus athericus	0.8	0.0017	1700	Rupprecht et al. (2017)
Phragmites australis	2.0	0.005	250	Schoutens et al. (2022)

flow resistance by vegetation. Annual average characteristics are included for each species to approximate seasonal variations in e.g. vegetation density and biomass, as these traits can change throughout the year (Marin-Diaz et al., 2023). For all vegetation species, a bulk drag coefficient of 1 was applied in the model for both calm-weather and storm conditions. This is a typical value for the drag coefficient of a rigid cylinder (Sonnenwald et al., 2019; Stone and Shen, 2002), and is commonly applied in modelling of vegetation resistance (Ashall et al., 2016; Baptist et al., 2007; Bennett et al., 2023; K. Hu et al., 2018).

From the vegetation maps, each polygon may consist of multiple vegetation species. Therefore, the weighted average characteristics are determined for each polygon. These weighted averages are imported in to the Delft3D-FM model by taking the weighted average again per grid cell of the model domain.

2.4. Analysis of model output

From the model output, particular attention is given to single tidal cycles: one during storm conditions and one during calm-weather conditions. During storm conditions, this includes the tidal cycle around the peak of the storm, resulting in the highest water levels due to both storm surge and spring tide. For comparison, a tidal cycle at the same phase within the spring-neap cycle - specifically, at spring tide-was selected during calm-weather conditions. The analysis of the impact of vegetation on currents focuses on peak ebb and peak flood velocities. These are essential parameters for characterizing tidal flow asymmetries, associated sediment dynamics, and subsequent morphological development. The phase difference in water levels and corresponding current velocities is accounted for in determining the peak ebb and flood velocities by extending the end of the flood phase with the phase difference in the direction of cross-sectionally averaged velocity. For more details, see Supplementary Materials A.

At first, zooms are presented on a few of the vegetated intertidal areas, both fringing and mid-channel flats, to study the impact on peak ebb and flood velocities on the marsh-mudflat scale. Subsequently, the different scenarios are compared based on the spatial scale of impact on peak ebb and peak flood velocities around the vegetated intertidal areas. This way, differences in excluding vegetation, including mono-specific vegetation and including multi-species vegetation are studied on an estuarine scale. Finally, model results for the 2016 snapshot of bathymetry and vegetation cover are compared with output of the 1993 snapshot. This focuses on the difference in peak ebb and flood velocities as modeled, isolating the effect of the bathymetrical and vegetation changes.

3. Results

3.1. Spatiotemporal vegetation dynamics

Between 1993 and 2016, the total extent of saltmarsh vegetation in the Western Scheldt increased from 2483 ha to 3350 ha. This increase occurred primarily between 1998 and 2010, while in recent years, the total extent of saltmarsh vegetation has stabilized (Fig. 2). However, this increase is neither equally distributed among the considered plant species nor consistent over time; only reed (*P. australis*) shows a continuous increase across all years.

By subtracting the 1993 vegetation map from that of 2016, the establishment, retreat and persistence of vegetation over these years becomes evident (Fig. 3). It is clearly seen that the increase in saltmarsh vegetation is primarily due to vegetation establishment on the mid-channel flats (Hooge Platen and Walsoorden); which transition from bare flats in 1993 to having an extensive vegetation cover in 2016. Furthermore, most flats on the north side of the estuary show a decrease in vegetation extent whereas most flats on the south side show an increase in extent.

The longitudinal (along-estuary) relative distribution of vegetation species (Fig. 4) is shown as normalized area per 10 km bin. As expected, more salt-tolerant species are found near the mouth, while less salt-tolerant species appear further up the estuary. A gradual change in relative species distribution is observed when moving further inland.

3.2. Local scale effects of vegetation on currents

Zooming in on several flats within the Western Scheldt allows for a comparison of the impact on currents on the vegetated marsh platforms and near surroundings (marsh-mudflat scale). From these zooms, a large reduction in current velocities is observed on the vegetated areas when compared to the no vegetation scenario, both during flooding and ebbing (10–80%). Furthermore, an increase in peak ebb and flood velocity is observed for some of the tidal creeks on the Saeftinghe marsh. In Supplementary Materials B, the absolute difference maps are presented. When examining the impact on peak flood velocity during storm conditions, differences between the mono-specific and multi-species vegetation scenarios become apparent. These differences are primarily present in the magnitude of the impact on velocities, rather than the extent around the vegetated zone. Especially on Saeftinghe, the type of vegetation appears to have an impact, with an even larger reduction in

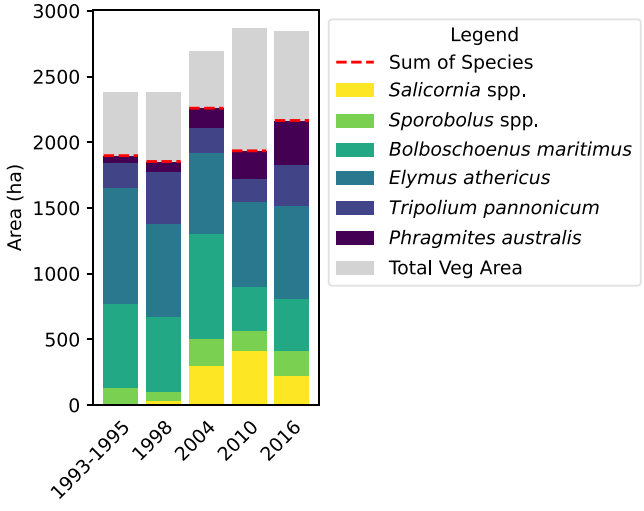

Fig. 2. Vegetation extent [ha] per species between 1993 and 2016. The bars indicate the total vegetated area per year with the dashed line representing the sum of the species considered in this study.

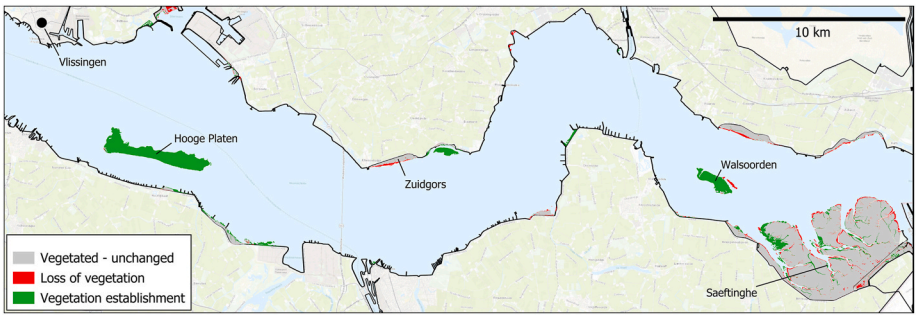

Fig. 3. Difference map of vegetation extent in the Western Scheldt between 1993 and 2016.

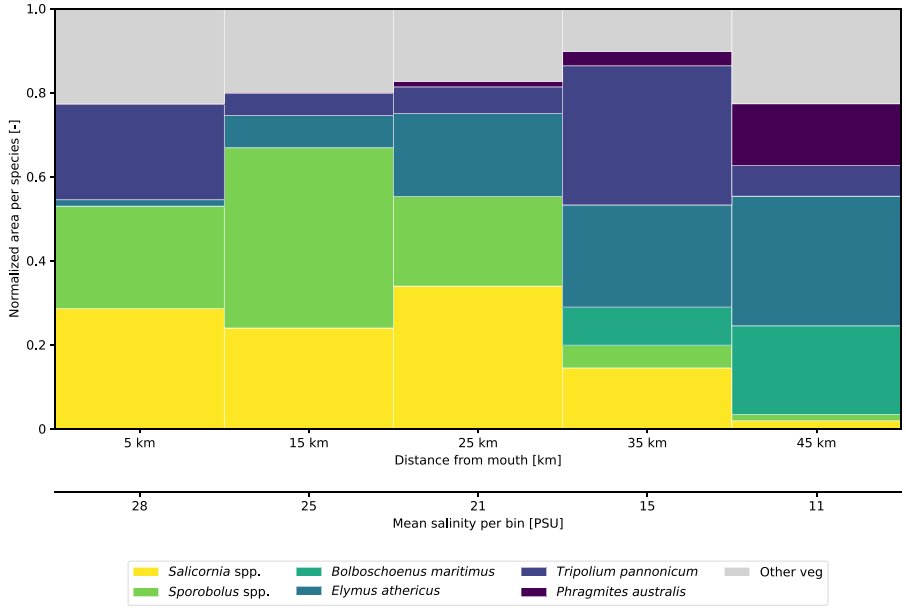

Fig. 4. Longitudinal vegetation distribution in 2016, presented as normalized area per species community for each 10 km bin when moving from the mouth (left, km 0) further upstream (right, km 50). Mean salinity is derived from a map provided by Rijkswaterstaat (modeled data of 1992).

current velocities over the vegetated area when including multiple species (Fig. 5). The Seaftinghe marsh is mainly covered by *Elymus athericus, Bolboschoenus maritimus, Phragmites australis* and some species not considered in this study. This diversity in species may explain the observed differences between the mono-specific and multi-species model runs. The difference between the mono-specific and multi-species vegetation is much smaller for Hooge Platen and Zuidgors, where the vegetation is dominated by *Sporobolus* spp., *Salicornia* spp., *Elymus athericus* and species not considered in this study. Therefore, the biomechanical properties of vegetation in the model are more similar in these areas, since the mono-specific vegetation characteristics are based on *Sporobolus* spp.

Results for the peak ebb velocities during storm conditions show a similar impact by the vegetation and, again, minor differences between the mono-specific and multi-species vegetation implementations (Fig. 6). Compared to the influence on peak flood velocities, the extent of the impact on ebb velocities is larger around the mid-channel flat Hooge Platen. Furthermore, the area of impact around the Saeftinghe marsh is more confined to the area next to the creeks, whereas during flooding this is mainly adjacent to the vegetated edge.

3.3. Spatial scale of hydrodynamic impact

On the estuarine scale (rather than the marsh-mudflat scale), in general, a minor effect of several percentage difference in the peak ebb and flood velocities is observed when including either mono-specific or multi-species vegetation (Fig. 7). In this study, peak flood velocities during the peak of the storm are lower compared to those during calm-weather conditions (Fig. 7a). This is due to the ebb water level prior to the peak water level during storm conditions being elevated by the storm surge. This is clearly visible in Supplementary Materials A.

During calm-weather conditions, the effect of vegetation on peak ebb and flood velocities is negligible on an estuarine scale (Fig. 8), in both relative and absolute terms (see Supplementary Materials B). However, a clear effect is still observed around the edge of the vegetation. In all scenarios (both storm and calm-weather conditions), the area of impact around the vegetation is observed to be in the order of magnitude of the vegetated extent or smaller.

The spatial extent of impact appears to be independent of vegetation parametrization: i.e. independent of including a single species (mono-specific vegetation) or multiple species (multi-species vegetation) in the model. Note that the differences on an estuarine scale are only a few percent. In Supplementary Materials D, the estuary-scale relative differences in peak ebb and peak flood velocities are presented as the 25th percentile, median and 75th percentile. In all model scenarios, both increases and decreases in peak ebb and flood velocity are observed. However, close to the vegetation edge of fringing flats, flood velocities are predominantly reduced, whereasebb velocities show an increase. This is most clearly observed around the Saeftinghe marsh. Furthermore, these effects are more pronounced during calm-weather conditions,

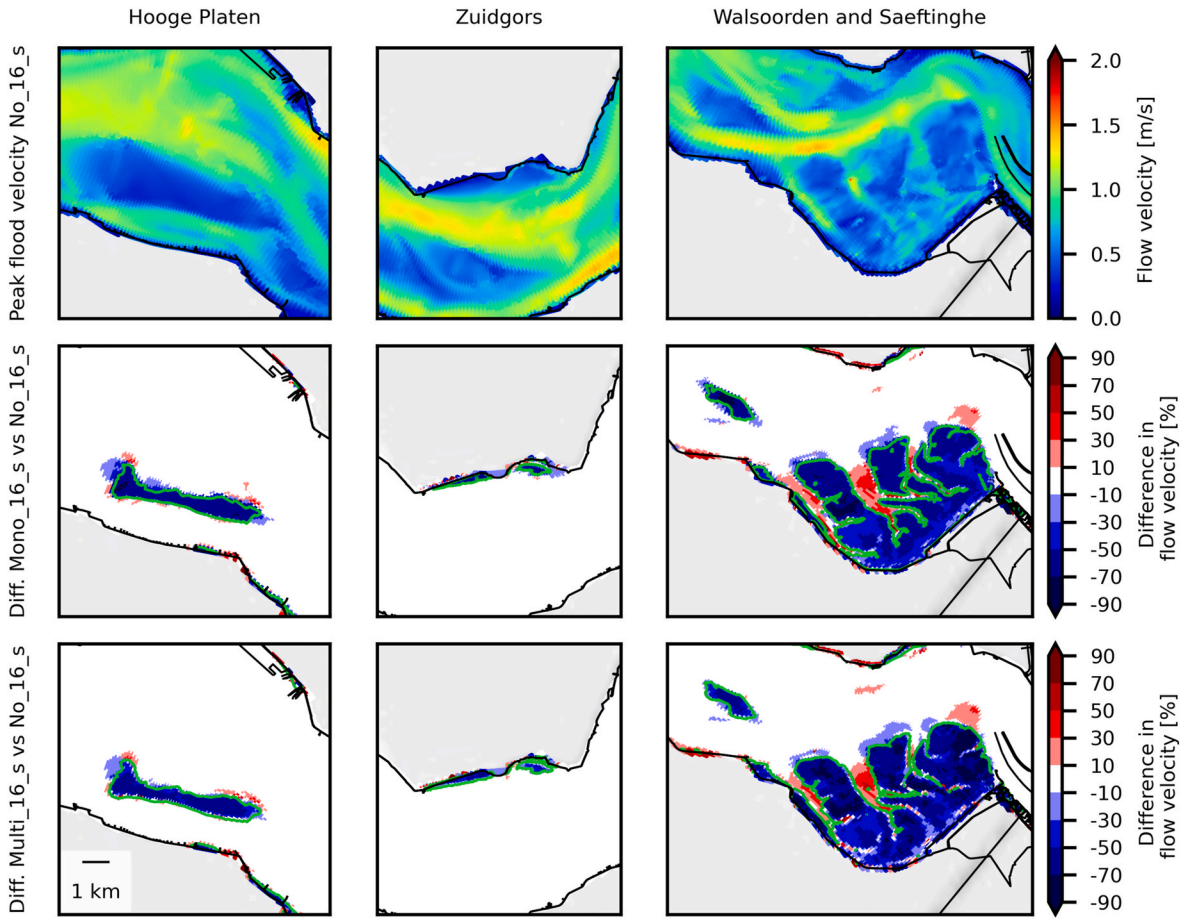

Fig. 5. Peak flood velocities during storm conditions for a zoom on Hooge Platen (left), Zuidgors (middle), and Walsoorden and Saeftinghe (right). The top panel shows the peak flood velocity for the no vegetation scenario, the middle panel the relative difference between the mono-specific and no vegetation scenario and the bottom panel the relative difference between the multi-species and the no vegetation scenario. The green contour represents the vegetation edge in the middle and lower panels.

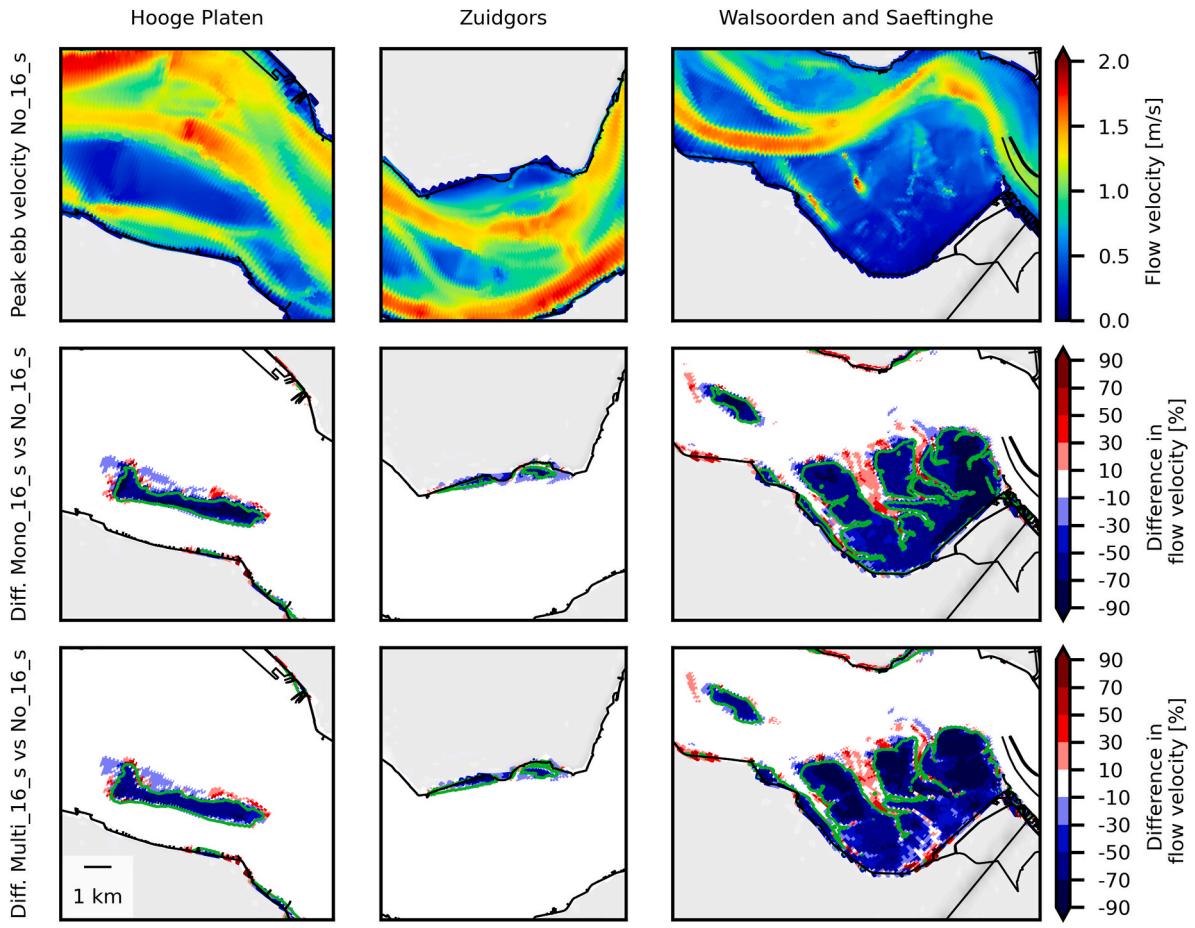

Fig. 6. Peak ebb velocities during storm conditions for a zoom on Hooge Platen (left), Zuidgors (middle), and Walsoorden and Saeftinghe (right). The top panel shows the peak ebb velocity for the no vegetation scenario, the middle panel the relative difference between the mono-specific and no vegetation scenario and the bottom panel the relative difference between the multi-species and the no vegetation scenario. The green contour represents the vegetation edge in the middle and lower panels.

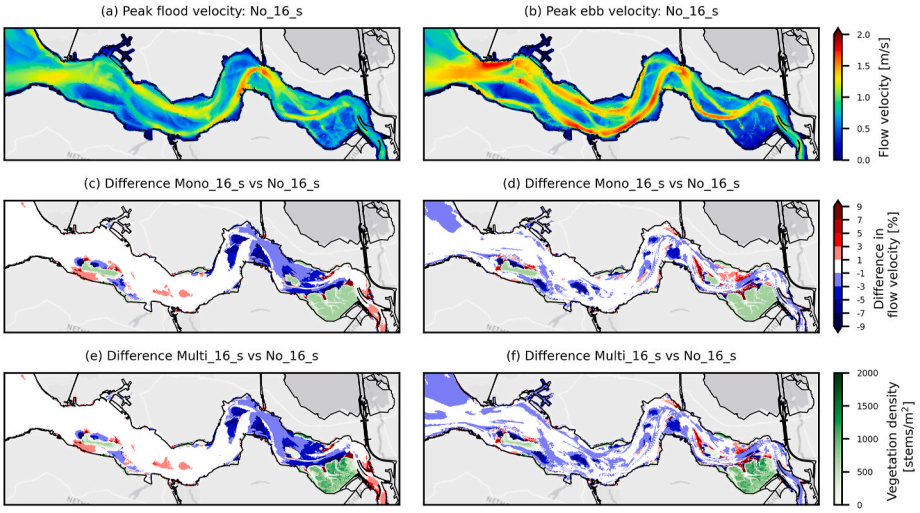

Fig. 7. Peak flood (a) and ebb (b) velocities during storm conditions for 2016 snapshots. In (c–d) the relative difference between the mono-specific vegetation and no vegetation scenario is shown. In (e–f) the relative difference between the multi-species vegetation and no vegetation scenario is shown. The colorbars for the difference in flow velocity and the vegetation density correspond to all subplots c-f.

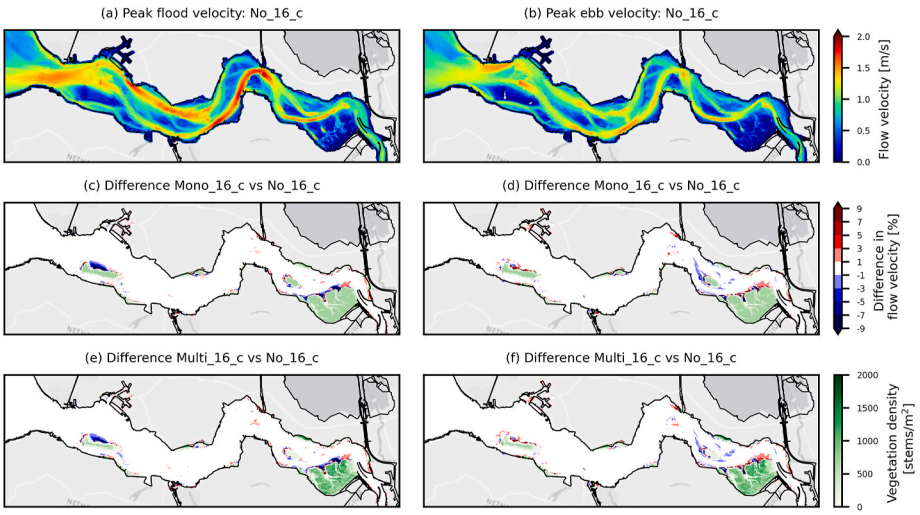

Fig. 8. Peak flood (a) and ebb (b) velocities during calm-weather conditions for 2016. In (c–d) the relative difference between the mono-specific vegetation and no vegetation scenario is shown. In (e–f) the relative difference between the multi-species vegetation and no vegetation scenario is shown. The colorbars for the difference in flow velocity and the vegetation density correspond to all subplots c-f.

whereas during storm conditions, greater spatial variation is observed. Besides the impact on peak flood and ebb velocities in the vicinity of saltmarsh vegetation, an impact is observed on shallow, non-vegetated areas. These can be distinguished by the low peak ebb and flood velocities (Fig. 7a–b).

3.4. *Bathymetry vs vegetation changes: which has a greater impact on currents?*

The effect of changes in bathymetry and vegetation cover on peak ebb and flood velocities are studied by comparing the 2016 snapshot of

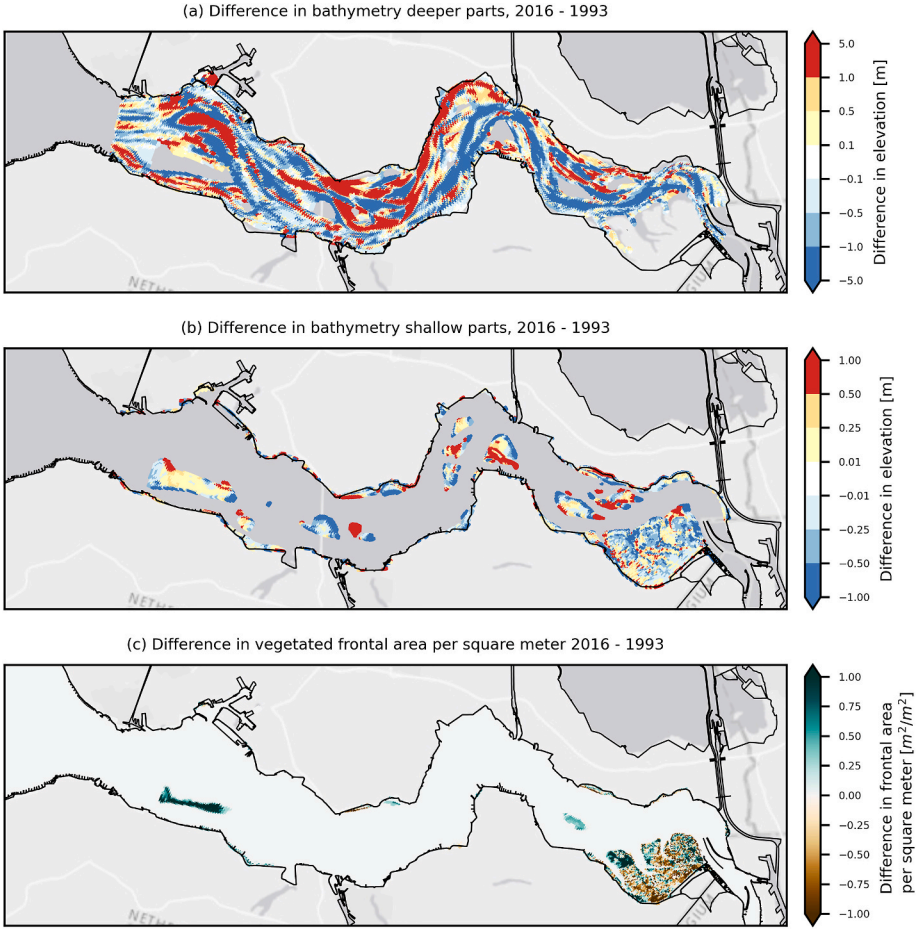

Fig. 9. Difference in bathymetry, with positive values indicating accretion and negative values erosion. Difference in bathymetry deeper parts (<0 m + NAP in both years) (a), difference in bathymetry shallow parts (>0 m + NAP in both years) (b) and difference in vegetated frontal area per square meter (c) computed as 2016–1993 based on the multi-species snapshots.

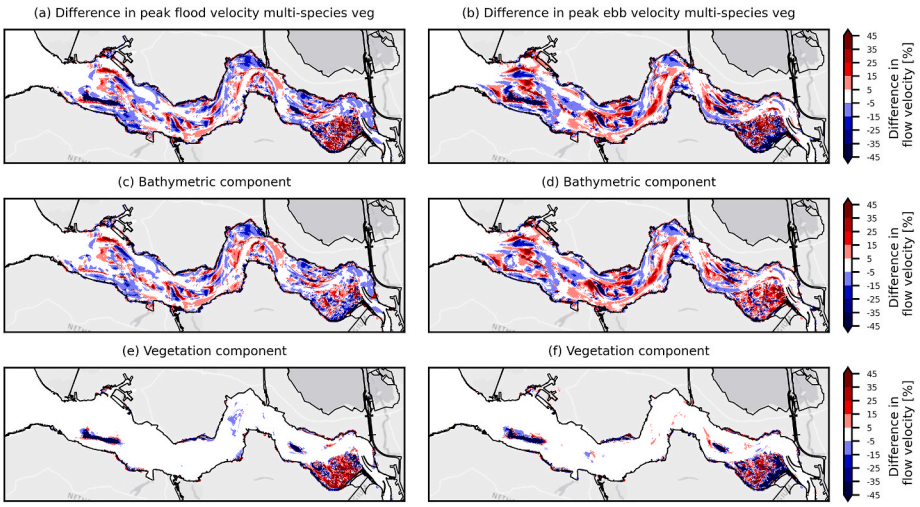

Fig. 10. Difference in peak flood (a) and ebb (b) velocities for the multi-species vegetation scenarios of 2016 and 1993. Panels (c) and (d) show the bathymetrical component of this difference and panels (e) and (f) the vegetation component.

bathymetry and vegetation cover with the 1993 snapshot. Bathymetrical changes between 1993 and 2016 reveal significant dynamics in the ebb and flood channels (Fig. 9a), showing accretion and erosion rates of several meters due to channel migration. On the shallower areas, spatial variations in erosion and accretion rates are observed, with magnitudes of up to ca 1 m (Fig. 9b). The largest changes occur close to the edge of the shallow areas. The largest changes in vegetated frontal area are found on the mid-channel flats, resulting from vegetation establishment between 1993 and 2016 (Fig. 9c). Furthermore, significant changes in vegetated frontal area are also observed on the fringing flats, driven by a combination of vegetation establishment, retreat and species composition changes.

The difference in peak ebb and flood velocities between 2016 and 1993 for the scenario with multi-species vegetation is shown in Fig. 10. Significant differences are observed in the deeper parts of the estuary, primarily due to the migration of ebb and flood channels. Presenting the bathymetric component and vegetation component separately allows for investigating the effect of bathymetrical changes and vegetation changes to the peak flood and ebb velocities. On the vegetated intertidal areas, contrasting effects of bathymetric and vegetation changes are observed for both the peak flood and ebb velocities. This is most evident on the Saeftinghe marsh, where the peak flood velocity predominantly increases. This increase is mainly due to changes in vegetation cover, since the bathymetrical changes actually caused a decrease in peak flood velocity.

The impact of vegetation establishment on the mid-channel flats Hooge Platen and Walsoorden is clearly seen in the vegetation component subfigures through the decrease in current velocities on the vegetated areas. In general, the impact of changes in vegetation cover is observed to be of the same order of magnitude as the impact due to changes in bathymetry over the period 1993–2016.

4. Discussion

In this study, we assessed the influence of vegetated intertidal areas on currents across different spatial scales within an estuarine environment. Our findings reveal that saltmarsh vegetation plays a crucial role in modulating currents, with its effects varying depending on the spatial scale. At broader estuarine scales, the presence of vegetation can be generalized, with mono-specific representations sufficiently capturing spatially extended effects on currents. However, at local marsh-mudflat scales, more detailed vegetation characteristics, including species-specific biomechanical properties, are essential to accurately represent the vegetation's influence on currents. This applies during both calm-weather and storm conditions, although the spatial extent of the impact on currents beyond the vegetated zone is almost negligible on an estuarine scale during calm-weather conditions. Between 1993 and 2016, we also found that within the vegetated area, bathymetrical changes and vegetation changes had a comparable magnitude of impact on altering current velocities. Given the highly dynamic nature of saltmarsh vegetation—characterized by significant temporal and spatial variations in cover and species distribution—our results underscore the importance of incorporating up-to-date and detailed vegetation data, particularly for models focusing on the marsh-mudflat scale.

4.1. Mono-specific vs multi-species vegetation

Saltmarsh vegetation reduces current velocities by inducing drag. This drag force depends on vegetation characteristics such as stem diameter, stem density and plant height. Gradients in environmental conditions lead to spatially varying plant species as well as inter-species variability in biomechanical properties. Therefore, the impact of vegetation on currents also varies spatially. From this study, it is observed that spatial variation is particularly important when assessing the impact of vegetation on currents at the scale of a marsh-mudflat system. In contrast, when studying estuary-scale hydrodynamics, spatial variation in vegetation species and corresponding biomechanical properties appears less relevant. However, these conclusions may depend on the ratio of vegetated intertidal area to the total estuary area. Bennett et al. (2023) found that in smaller estuaries with a higher ratio of vegetated intertidal area, the frictional drag exerted by vegetation can reduce tidal amplitudes and residual currents. Their study focused on mono-specific vegetation, highlighting the potential value of comparing these findings with those from multi-species vegetation in similar estuarine environments. However, the differences in the modeled impact on currents between mono-specific and multi-species vegetation depend on the species present. When the biomechanical properties of the species in a multi-species community are similar to those used in a mono-specific approach, only minor differences in model outcomes are expected. However, even when using mono-specific vegetation in models, it is essential to have a basic understanding of the vegetation's characteristics, such as those defined at the ecotope level, to ensure accurate results. Furthermore, the inclusion of mono-specific or multi-species vegetation is study area dependent. When the range of vegetation species and corresponding biomechanical characteristics is large (e.g. from grasses like Glasswort to trees like Willows), a mono-specific vegetation implementation might not provide an accurate estimate of the vegetation impact, even at the estuarine scale.

4.2. Seasonal variability in vegetation impact

Our results indicate that the impact of saltmarsh vegetation on currents is less pronounced during calm-weather conditions compared to storm conditions, both in magnitude and spatial extent. However, it is important to note that in this study, vegetation characteristics were modeled as static and independent of the varying forcing conditions. In reality, storminess is typically more prevalent during autumn and winter months, when vegetation usually has different characteristics compared to summer (or even dies off). This affects the drag exerted by the vegetation and, therefore, influences current velocities. Additionally, during a storm, vegetation can experience damage (e.g. stem breakage) or in the case of flexible vegetation it can bend, reducing the frontal area (Paul et al., 2016; Rupprecht et al., 2017; Vuik et al., 2018). Both result in a smaller impact on current velocities during storm conditions. Moreover, during storms, the water levels are elevated, reducing the ratio of plant height to water depth (submergence ratio), which decreases hydrodynamic energy dissipation (Maza et al., 2015). However, at the same time, the elevated water levels cause the intertidal areas to be inundated completely, thereby increasing the extent of vegetated intertidal area impacting the flow field. During calm-weather conditions, this is not the case (at least not in our study area). Next, the vegetated areas remain inundated for a longer part of the tidal cycle compared to calm-weather conditions. This makes that the vegetated zone contributing to the flow carrying width of the estuary is larger during storm conditions.

4.3. Biogeomorphological interactions

Our results indicate that changes in bathymetry and vegetation cover both significantly affect currents. In the comparison between two snapshots (combination of bathymetry and vegetation cover at a single moment in time) neither factor can be neglected, as the impact of changes are estimated to be of a similar order of magnitude. Moreover, they can have opposing effects, for example, a change in bathymetry might increase peak ebb or peak flood velocities, while the change in vegetation cover could decrease it, or vice versa. Although treated separately in this paper, vegetation cover, bathymetrical changes and hydrodynamics are interconnected through biogeomorphological interactions, together shaping wetland landscapes (Schwarz et al., 2018). Such interactions are crucial for understanding long-term changes in vegetation and geomorphology (Feng et al., 2025). While this study considers static snapshots of vegetation and bathymetry, succession introduces a dynamic component over multi-year timescales, influencing both marsh-mudflat and estuarine-scale interactions. By incorporating these longer-term successional dynamics into models, we can better anticipate gradual changes in estuarine morphology and hydrodynamic behavior. One implication of this can be that, although vegetation does not seem to impact currents on an estuarine scale, at the marsh-mudflat scale hydrodynamic impact might result in changes to the geomorphology of the estuary, thereby indirectly influencing currents at the estuarine scale. So far, biogeomorphological modelling is usually performed on a marsh-mudflat scale (Best et al., 2018; Fagherazzi et al., 2012; Schwarz et al., 2018; Willemsen et al., 2022). However, estuary scale biogeomorphological modelling could enhance our understanding of the evolution of estuaries, especially under changing environmental conditions (Siemes et al., 2024).

Additionally, this study employed a 2D model focusing solely on currents, excluding waves, wave-current interactions, and 3D hydrodynamic effects. However, wave action plays a key role in sediment resuspension and transport, influencing sediment availability for plant establishment and stability. Wave-current interactions can affect vegetation anchoring and growth, while denser vegetation can dampen waves and foster sediment accumulation, supporting succession. Including 3D hydrodynamics would allow for a more detailed representation of velocity gradients across the water column, particularly in areas with sharp transitions in bathymetry and vegetation density. By integrating 3D models and wave effects, future research could better capture the feedback between hydrodynamics and vegetation, improving our understanding of long-term biogeomorphological interactions.

4.4. Retrieving vegetation information

Accurately defining the extent and biomechanical characteristics of saltmarsh vegetation for model parameterization is challenging due to the complexity of natural environments. Spatial heterogeneity, difficulties in field measurements, and the dynamic nature of vegetation across different seasons and years further complicate this task. Remote sensing techniques offer a potential solution by enabling large-scale mapping of the extent and dynamics of saltmarsh area (Laengner et al., 2019), saltmarsh plant species or vegetation community (e.g. Belluco et al., 2006), as well as retrieving vegetation characteristics such as Leaf Area Index (Oteman et al., 2019). Maza et al. (2022) found that the mean meadow height and aboveground biomass of marsh vegetation are good proxies for its wave attenuating capacity, and can be derived by remote sensing techniques. However, retrieving plant-specific characteristics like the stem diameter by remote sensing techniques remains a challenge.

4.5. Nature-based solutions

Given the growing interest in incorporating nature-based solutions for various purposes (e.g. coastal protection, salt intrusion mitigation, erosion prevention), a thorough understanding of biogeomorphological interactions is essential. The impact on current velocities on and around the vegetated intertidal areas, as shown in this study, are especially important for the sake of coastal protection and erosion prevention. However, from a salt intrusion perspective, estuary scale impacts are more relevant (Hendrickx et al., 2023; Hendrickx and Pearson, 2024; Siemes, 2024). On this estuarine scale, the vegetation cover itself may not significantly influence estuarine hydrodynamics. However, the extent of intertidal area can have a substantial impact on this scale. In other words, changes in intertidal areas within the current estuary boundaries have a limited effect on estuarine hydrodynamics, whereas modifications to intertidal areas outside the current boundaries—such as through managed realignment or land claim—can significantly alter the tidal prism, water levels and flow structure (Bennett et al., 2020; Siemes et al., 2024; Stark et al., 2017b; Weisscher et al., 2022). Moreover, incorporating vegetation in nature-based solution can offer benefits for erosion prevention, and therefore resilience, of the solution in place. To maximize the effectiveness of nature-based solutions, it is important to consider adaptive management strategies that account for both short-term and long-term changes in vegetation and sediment dynamics. Ongoing monitoring of these systems is crucial for understanding the evolving interactions between biotic and abiotic factors and for refining models that strive to predict the outcomes of such interventions. One example of such an approach is the study by Brunink and Hendrickx (2024), who predicted ecotopes based on model output from a hydrodynamic model. This can aid in the prediction of ecological shifts resulting from changes in hydrodynamics when implementing nature-based solutions.

5. Conclusions

This study quantified how and over which spatial scale vegetated intertidal areas influence estuarine currents and examined the temporal variation caused by changes in vegetation cover. These changes were most prominent on the mid-channel flats of the Scheldt estuary. Vegetation establishment on these mid-channel flats contributed to an overall increase in saltmarsh area within the estuary (2483 ha–3350 ha from 1993 to 2016). The species distribution generally corresponds to the

streamwise salinity distribution. Using a Delft3D-FM model schematization of the Scheldt estuary, we demonstrated that saltmarsh vegetation reduces both ebb and flood peak velocities (10–80% within the vegetated zone and 1–30% around the vegetated zone), both during calm-weather and storm conditions. In this, both magnitude and extent of impact are smaller during calm-weather conditions compared to storm conditions. The influence on current velocities extends beyond the vegetated edge during storm conditions, typically over an area comparable to or smaller than the size of the vegetated zone, whereas the impact is limited to the vegetated zone during calm-weather conditions. On this estuarine scale, the spatial extent of impact appears independent of vegetation parametrization, with no significant difference between mono-specific and multi-species vegetation. However, at the smaller marsh-mudflat scale, the inclusion of multiple species leads to a different spatial pattern in the magnitude of impact within the vegetated area, while the spatially extended effects remain similar. Furthermore, decadal-scale variations in vegetation extent and distribution were found to impact current velocities to a similar order of magnitude as changes in bathymetry over the same period. These findings emphasize the importance of saltmarsh vegetation's influence on currents at the marsh-mudflat scale in particular.

CRediT authorship contribution statement

Jesse Bootsma: Writing – original draft, Visualization, Methodology, Investigation, Formal analysis, Conceptualization. **Bas W. Borsje:** Writing – review & editing, Supervision, Methodology, Conceptualization. **Daphne van der Wal:** Writing – review & editing, Supervision, Methodology, Conceptualization. **Suzanne J.M.H. Hulscher:** Writing – review & editing, Supervision, Project administration, Funding acquisition, Conceptualization.

Data availability

Vegetation maps (https://maps.rijkswaterstaat.nl/dataregister/srv/dut/catalog.search#/metadata/0bb7f390-7761-41da-b341-828c1bc74b5c) and bathymetry data (https://maps.rijkswaterstaat.nl/dataregister/srv/dut/catalog.search#/metadata/07de2e41-ac5d-41d9-9c3c-bfdd502a4069).

Funding sources

This publication is part of the project "Design and operation of nature-based SALTISolutions" (with project number P18-32 Project 7) of the research programme SALTISolutions which is (partly) financed by the Dutch Research Council (NWO).

Declaration of competing interest

The authors declare that they have no known competing financial interests or personal relationships that could have appeared to influence the work reported in this paper.

Acknowledgements

This work is part of the Perspectief Program SALTISolutions, which is funded by NWO Domain Applied and Engineering Sciences in collaboration with private and public partners. We thank Deltares for their help with the NeVla model, Rijkswaterstaat for providing vegetation and bathymetry data and Jing Feng for discussions on data analysis and visualization. This work used the Dutch national e-infrastructure with the support of the SURF Cooperative.

Appendix A. Supplementary data

Supplementary data to this article can be found online at https://doi.org/10.1016/j.ecss.2025.109177.

Data availability

Data will be made available on request.

References

Ashall, L.M., Mulligan, R.P., Van Proosdij, D., Poirier, E., 2016. Application and validation of a three-dimensional hydrodynamic model of a macrotidal salt marsh. Coast. Eng. 114, 35–46. https://doi.org/10.1016/j.coastaleng.2016.04.005.

Baeyens, W., Van Eck, B., Lambert, C., Wollast, R., Goeyens, L., 1997. General description of the Scheldt estuary. Hydrobiologia 366 (1–3), 1–14. https://doi.org/10.1023/a:1003164009031.

Baptist, M.J., Babovic, V., Uthurburu, J.R., Keijzer, M., Uittenbogaard, R.E., Mynett, A., Verwey, A., 2007. On inducing equations for vegetation resistance. J. Hydraul. Res. 45 (4), 435–450. https://doi.org/10.1080/00221686.2007.9521778.

Barbier, E.B., Hacker, S.D., Kennedy, C., Koch, E.W., Stier, A.C., Silliman, B.R., 2011. The value of estuarine and coastal ecosystem services. Ecol. Monogr. 81 (2), 169–193. https://doi.org/10.1890/10-1510.1.

Belluco, E., Camuffo, M., Ferrari, S., Modenese, L., Silvestri, S., Marani, A., Marani, M., 2006. Mapping salt-marsh vegetation by multispectral and hyperspectral remote sensing. Remote Sens. Environ. 105 (1), 54–67. https://doi.org/10.1016/j.rse.2006.06.006.

Bennett, W.G., Horrillo-caraballo, J.M., Fairchild, T.P., Veelen, T. J. Van, Karunarathna, H., 2023. Saltmarsh vegetation alters tidal hydrodynamics of small estuaries. Appl. Ocean Res. 138 (February), 103678. https://doi.org/10.1016/j.apor.2023.103678.

Bennett, W.G., van Veelen, T.J., Fairchild, T.P., Griffin, J.N., Karunarathna, H., 2020. Computational modelling of the impacts of saltmarsh management interventions on hydrodynamics of a small macro-tidal estuary. J. Mar. Sci. Eng. 8 (5). https://doi.org/10.3390/JMSE8050373.

Best, S.N., Van der Wegen, M., Dijkstra, J., Willemsen, P.W.J.M., Borsje, B.W., Roelvink, D.J.A., 2018. Do salt marshes survive sea level rise? Modelling wave action, morphodynamics and vegetation dynamics. Environ. Model. Software 109 (August), 152–166. https://doi.org/10.1016/j.envsoft.2018.08.004.

Borsje, B.W., van Wesenbeeck, B.K., Dekker, F., Paalvast, P., Bouma, T.J., van Katwijk, M.M., de Vries, M.B., 2011. How ecological engineering can serve in coastal protection. Ecol. Eng. 37 (2), 113–122. https://doi.org/10.1016/j.ecoleng.2010.11.027.

Bouma, T.J., De Vries, M.B., Low, E., Kusters, L., Herman, P.M.J., Tánczos, I.C., Temmerman, S., Hesselink, A., Meire, P., Van Regenmortel, S., 2005a. Flow hydrodynamics on a mudflat and in salt marsh vegetation: identifying general relationships for habitat characterisations. Hydrobiologia 540 (1–3), 259–274. https://doi.org/10.1007/s10750-004-7149-0.

Bouma, T.J., De Vries, M.B., Low, E., Peralta, G., Tánczos, I.C., Van De Koppel, J., Herman, P.M.J., 2005b. Trade-offs related to ecosystem engineering: a case study on stiffness of emerging macrophytes. Ecology 86 (8), 2187–2199. https://doi.org/10.1890/04-1588.

Bouma, T.J., Temmerman, S., van Duren, L.A., Martini, E., Vandenbruwaene, W., Callaghan, D.P., Balke, T., Biermans, G., Klaassen, P.C., van Steeg, P., Dekker, F., van de Koppel, J., de Vries, M.B., Herman, P.M.J., 2013. Organism traits determine the strength of scale-dependent bio-geomorphic feedbacks: a flume study on three intertidal plant species. Geomorphology 180–181, 57–65. https://doi.org/10.1016/j.geomorph.2012.09.005.

Bouma, T.J., van Belzen, J., Balke, T., Zhu, Z., Airoldi, L., Blight, A.J., Davies, A.J., Galvan, C., Hawkins, S.J., Hoggart, S.P.G., Lara, J.L., Losada, I.J., Maza, M., Ondiviela, B., Skov, M.W., Strain, E.M., Thompson, R.C., Yang, S., Zanuttigh, B., et al., 2014. Identifying knowledge gaps hampering application of intertidal habitats in coastal protection: opportunities & steps to take. Coast. Eng. 87, 147–157. https://doi.org/10.1016/j.coastaleng.2013.11.014.

Breine, J., Maes, J., Stevens, M., Simoens, I., Elliott, M., Hemingway, K., Van den Bergh, E., 2008. Water management strategies for estuarine and transitional waters in the North Sea Region. HARBASINS : Harmonised River Basin Strategies North Sea Habitat Needs to Realise Conservation Goals for Fish in Estuaries : Case Study of the Tidal Schelde. Rapport van Het Instituut Voor Natuur- En Bosonderzoek.

Brooks, H., Möller, I., Carr, S., Chirol, C., Christie, E., Evans, B., Spencer, K.L., Spencer, T., Royse, K., 2021. Resistance of salt marsh substrates to near-instantaneous hydrodynamic forcing. Earth Surf. Process. Landforms 46 (1), 67–88. https://doi.org/10.1002/esp.4912.

Brunink, S., Hendrickx, G.G., 2024. Predicting ecotopes from hydrodynamic model data: towards an ecological assessment of nature-based solutions. Nature-Based Solutions 6 (June), 100145. https://doi.org/10.1016/j.nbsj.2024.100145.

Cahoon, D.R., McKee, K.L., Morris, J.T., 2021. How plants influence resilience of salt marsh and mangrove wetlands to sea-level rise. Estuaries Coasts 44 (4), 883–898. https://doi.org/10.1007/s12237-020-00834-w.

Campbell, A.D., Fatoyinbo, L., Goldberg, L., Lagomasino, D., 2022. Global hotspots of salt marsh change and carbon emissions. Nature 612 (7941), 701–706. https://doi.org/10.1038/s41586-022-05355-z.

Carrion Aretxabala, B., 2015. Morphological Impact of the Sinterklaas Storm at Het Zwin: Numerical Modelling with XBeach, vol. 75.

Crain, C.M., Silliman, B.R., Bertness, S.L., Bertness, M.D., 2004. Physical and biotic drivers of plant distribution across estuarine salinity gradients. Ecology 85 (9), 2539–2549. https://doi.org/10.1890/03-0745.

Fagherazzi, S., Kirwan, M.L., Mudd, S.M., Guntenspergen, G.R., Temmerman, S., D'Alpaos, A., Van De Koppel, J., Rybczyk, J.M., Reyes, E., Craft, C., Clough, J., 2012. Numerical models of salt marsh evolution: ecological, geomorphic, and climatic factors. Rev. Geophys. 50 (1), 1–28. https://doi.org/10.1029/2011RG000359.

Fairchild, T.P., Bennett, W.G., Smith, G., Day, B., Skov, M.W., Möller, I., Beaumont, N., Karunarathna, H., Griffin, J.N., 2021. Coastal wetlands mitigate storm flooding and associated costs in estuaries. Environ. Res. Lett. 16 (7). https://doi.org/10.1088/1748-9326/ac0c45.

Feng, J., Grandjean, T.J., Van de Koppel, J., Van der Wal, D., 2025. A spatiotemporal framework to assess the bio-geomorphic interplay of saltmarsh vegetation and tidal emergence (Western Scheldt estuary). Int. J. Appl. Earth Obs. Geoinf. 136, 104337. https://doi.org/10.1016/j.jag.2024.104337.

Guerra-Chanis, G.E., Laurel-Castillo, J.A., Schettini, C.A.F., Kakoulaki, G., Souza, A.J., Valle-Levinson, A., 2022. Saltwater intrusion in estuaries with different dynamic depths. Regional Studies in Marine Science 51, 102186. https://doi.org/10.1016/j.rsma.2022.102186.

Hendrickx, G.G., Kranenburg, W.M., Antolínez, J.A.A., Huismans, Y., Aarninkhof, S.G.J., Herman, P.M.J., 2023. Sensitivity of salt intrusion to estuary-scale changes: a systematic modelling study towards nature-based mitigation measures. Estuar. Coast Shelf Sci. 295 (April), 108564. https://doi.org/10.1016/j.ecss.2023.108564.

Hendrickx, G.G., Pearson, S.G., 2024. On the effects of intertidal area on estuarine salt intrusion. J. Geophys. Res.: Oceans 129 (9), 1–12. https://doi.org/10.1029/2023JC020750.

Hu, K., Chen, Q., Wang, H., Hartig, E.K., Orton, P.M., 2018. Numerical modeling of salt marsh morphological change induced by Hurricane Sandy. Coast. Eng. 132, 63–81. https://doi.org/10.1016/j.coastaleng.2017.11.001. January 2017.

Hu, Z., Van Belzen, J., Van Der Wal, D., Balke, T., Wang, Z.B., Stive, M., Bouma, T.J., 2015. Windows of opportunity for salt marsh vegetation establishment on bare tidal flats: the importance of temporal and spatial variability in hydrodynamic forcing. J. Geophys. Res.: Biogeosciences 120 (7), 1450–1469. https://doi.org/10.1002/2014JG002870.

Hu, Z., van der Wal, D., Cai, H., van Belzen, J., Bouma, T.J., 2018. Dynamic equilibrium behaviour observed on two contrasting tidal flats from daily monitoring of bed-level changes. Geomorphology 311, 114–126. https://doi.org/10.1016/j.geomorph.2018.03.025.

Jones, C.G., Lawton, J.H., Shachak, M., 1994. Organisms as ecosystem engineers. Oikos 69 (3), 373. https://doi.org/10.2307/3545850.

Koch, E.W., Barbier, E.B., Silliman, B.R., Reed, D.J., Perillo, G.M.E., Hacker, S.D., Granek, E.F., Primavera, J.H., Muthiga, N., Polasky, S., Halpern, B.S., Kennedy, C.J., Kappel, C.V., Wolanski, E., 2009. Non-linearity in ecosystem services: temporal and spatial variability in coastal protection. Front. Ecol. Environ. 7 (1), 29–37. https://doi.org/10.1890/080126.

Laengner, M.L., Siteur, K., van der Wal, D., 2019. Trends in the seaward extent of saltmarshes across Europe from long-term satellite data. Remote Sens. 11 (14), 1–25. https://doi.org/10.3390/rs11141653.

Leonard, L.A., Croft, A.L., 2006. The effect of standing biomass on flow velocity and turbulence in Spartina alterniflora canopies. Estuar. Coast Shelf Sci. 69 (3–4), 325–336. https://doi.org/10.1016/j.ecss.2006.05.004.

Leonard, L.A., Luther, M.E., 1995. Flow hydrodynamics in tidal marsh canopies. Limnol. Oceanogr. 40 (8), 1474–1484. https://doi.org/10.4319/lo.1995.40.8.1474.

Leonard, L.A., Reed, D.J., 2002. Hydrodynamics and sediment transport through tidal marsh canopies. J. Coast Res. 36 (October), 459–469. https://doi.org/10.2112/1551-5036-36.sp1.459.

Marin-Diaz, B., van der Wal, D., Kaptein, L., Martinez-Garcia, P., Lashley, C.H., de Jong, K., Nieuwenhuis, J.W., Govers, L.L., Olff, H., Bouma, T.J., 2023. Using salt marshes for coastal protection: effective but hard to get where needed most. J. Appl. Ecol. 60 (7), 1286–1301. https://doi.org/10.1111/1365-2664.14413.

Maza, M., Lara, J.L., Losada, I.J., 2022. A paradigm shift in the quantification of wave energy attenuation due to saltmarshes based on their standing biomass. Sci. Rep. 12 (1), 13883. https://doi.org/10.1038/s41598-022-18143-6.

Maza, M., Lara, J.L., Losada, I.J., Ondiviela, B., Trinogga, J., Bouma, T.J., 2015. Large-scale 3-D experiments of wave and current interaction with real vegetation. Part 2: experimental analysis. Coast. Eng. 106, 73–86. https://doi.org/10.1016/j.coastaleng.2015.09.010.

McLeod, E., Chmura, G.L., Bouillon, S., Salm, R., Björk, M., Duarte, C.M., Lovelock, C.E., Schlesinger, W.H., Silliman, B.R., 2011. A blueprint for blue carbon: toward an improved understanding of the role of vegetated coastal habitats in sequestering CO2. Front. Ecol. Environ. 9 (10), 552–560. https://doi.org/10.1890/110004.

Meire, P., Ysebaert, T., Van Damme, S., Van Den Bergh, E., Maris, T., Struyf, E., 2005. The Scheldt estuary: a description of a changing ecosystem. Hydrobiologia 540 (1–3), 1–11. https://doi.org/10.1007/s10750-005-0896-8.

Möller, I., Kudella, M., Rupprecht, F., Spencer, T., Paul, M., Van Wesenbeeck, B.K., Wolters, G., Jensen, K., Bouma, T.J., Miranda-Lange, M., Schimmels, S., 2014. Wave attenuation over coastal salt marshes under storm surge conditions. Nat. Geosci. 7 (10), 727–731. https://doi.org/10.1038/NGEO2251.

Morris, R.L., Konlechner, T.M., Ghisalberti, M., Swearer, S.E., 2018. From grey to green: efficacy of eco-engineering solutions for nature-based coastal defence. Glob. Change Biol. 24 (5), 1827–1842. https://doi.org/10.1111/gcb.14063.

Narayan, S., Beck, M.W., Reguero, B.G., Losada, I.J., Van Wesenbeeck, B., Pontee, N., Sanchirico, J.N., Ingram, J.C., Lange, G.M., Burks-Copes, K.A., 2016. The effectiveness, costs and coastal protection benefits of natural and nature-based defences. PLoS One 11 (5), 1–17. https://doi.org/10.1371/journal.pone.0154735.

Nepf, H.M., 1999. Drag, turbulence, and diffusion in flow through emergent vegetation. Water Resour. Res. 35 (2), 479–489. https://doi.org/10.1029/1998WR900069.

Neubauer, S.C., 2013. Ecosystem responses of a tidal freshwater marsh experiencing saltwater intrusion and altered hydrology. Estuaries Coasts 36 (3), 491–507. https://doi.org/10.1007/s12237-011-9455-x.

Neumeier, U., 2007. Velocity and turbulence variations at the edge of saltmarshes. Cont. Shelf Res. 27 (8), 1046–1059. https://doi.org/10.1016/j.csr.2005.07.009.

Neumeier, U., Amos, C.L., 2006. The influence of vegetation on turbulence and flow velocities in European salt-marshes. Sedimentology 53 (2), 259–277. https://doi.org/10.1111/j.1365-3091.2006.00772.x.

Oteman, B., Morris, E.P., Peralta, G., Bouma, T.J., van derWal, D., 2019. Using remote sensing to identify drivers behind spatial patterns in the bio-physical properties of a saltmarsh pioneer. Remote Sens. 11 (5). https://doi.org/10.3390/rs11050511.

Paul, M., Rupprecht, F., Möller, I., Bouma, T.J., Spencer, T., Kudella, M., Wolters, G., van Wesenbeeck, B.K., Jensen, K., Miranda-Lange, M., Schimmels, S., 2016. Plant stiffness and biomass as drivers for drag forces under extreme wave loading: a flume study on mimics. Coast. Eng. 117, 70–78. https://doi.org/10.1016/j.coastaleng.2016.07.004.

Pennings, S.C., Grant, M.B., Bertness, M.D., 2005. Plant zonation in low-latitude salt marshes: disentangling the roles of flooding, salinity and competition. J. Ecol. 93 (1), 159–167. https://doi.org/10.1111/j.1365-2745.2004.00959.x.

Rupprecht, F., Möller, I., Paul, M., Kudella, M., Spencer, T., van Wesenbeeck, B.K., Wolters, G., Jensen, K., Bouma, T.J., Miranda-Lange, M., Schimmels, S., 2017. Vegetation-wave interactions in salt marshes under storm surge conditions. Ecol. Eng. 100, 301–315. https://doi.org/10.1016/j.ecoleng.2016.12.030.

Schoutens, K., Stoorvogel, M., van den Berg, M., van den Hoven, K., Bouma, T.J., Aarninkhof, S., Herman, P.M.J., van Loon-Steensma, J.M., Meire, P., Schoelynck, J., Peeters, P., Temmerman, S., 2022. Stability of a tidal marsh under very high flow velocities and implications for nature-based flood defense. Front. Mar. Sci. 9 (July), 1–16. https://doi.org/10.3389/fmars.2022.920480.

Schwarz, C., Gourgue, O., van Belzen, J., Zhu, Z., Bouma, T.J., van de Koppel, J., Ruessink, G., Claude, N., Temmerman, S., 2018. Self-organization of a biogeomorphic landscape controlled by plant life-history traits. Nat. Geosci. 11 (9), 672–677. https://doi.org/10.1038/s41561-018-0180-y.

Shi, B.W., Yang, S.L., Wang, Y.P., Bouma, T.J., Zhu, Q., 2012. Relating accretion and erosion at an exposed tidal wetland to the bottom shear stress of combined current-wave action. Geomorphology 138 (1), 380–389. https://doi.org/10.1016/j.geomorph.2011.10.004.

Siemes, R.W.A., 2024. Modelling the effect of human interventions and climate change impacts on the sediment balance and salt intrusion in engineered estuaries. PhD thesis University of Twente. https://doi.org/10.3990/1.9789036562591.

Siemes, R.W.A., Duong, T.M., Borsje, B.W., Hulscher, S.J.M.H., 2024. Climate change can intensify the effects of local interventions: a morphological modeling study of a highly engineered estuary. J. Geophys. Res.: Earth Surf. 129 (7). https://doi.org/10.1029/2023JF007595.

Silliman, B.R., He, Q., Angelini, C., Smith, C.S., Kirwan, M.L., Daleo, P., Renzi, J.J., Butler, J., Osborne, T.Z., Nifong, J.C., van de Koppel, J., 2019. Field experiments and meta-analysis reveal wetland vegetation as a crucial element in the coastal protection paradigm. Curr. Biol. 29 (11), 1800–1806.e3. https://doi.org/10.1016/j.cub.2019.05.017.

Sonnenwald, F., Stovin, V., Guymer, I., 2019. Estimating drag coefficient for arrays of rigid cylinders representing emergent vegetation. J. Hydraul. Res. 57 (4), 591–597. https://doi.org/10.1080/00221686.2018.1494050.

Stark, J., Meire, P., Temmerman, S., 2017a. Changing tidal hydrodynamics during different stages of eco-geomorphological development of a tidal marsh: a numerical modeling study. Estuar. Coast Shelf Sci. 188, 56–68. https://doi.org/10.1016/j.ecss.2017.02.014.

Stark, J., Smolders, S., Meire, P., Temmerman, S., 2017b. Impact of intertidal area characteristics on estuarine tidal hydrodynamics: a modelling study for the Scheldt Estuary. Estuar. Coast Shelf Sci. 198, 138–155. https://doi.org/10.1016/j.ecss.2017.09.004.

Stark, J., Smolders, S., Vandenbruwaene, W., Mostaert, F., 2020. Agenda for the Future – historical evolution of tides and morphology in the Scheldt Estuary: sub report 4. Hydrodynamic modelling of morphological scenarios, 14_147_4. http://documentatiecentrum.watlab.be/owa/imis.php?module=ref&refid=322162.

Stone, B.M., Shen, H.T., 2002. Hydraulic resistance of flow in channels with cylindrical roughness. J. Hydraul. Eng. 128 (5), 500–506. https://doi.org/10.1061/(asce)0733-9429(2002)128:5(500.

Sutton-Grier, A.E., Wowk, K., Bamford, H., 2015. Future of our coasts: the potential for natural and hybrid infrastructure to enhance the resilience of our coastal communities, economies and ecosystems. Environ. Sci. Pol. 51 (August), 137–148. https://doi.org/10.1016/j.envsci.2015.04.006.

Temmerman, S., Bouma, T.J., Govers, G., Wang, Z.B., De Vries, M.B., Herman, P.M.J., 2005. Impact of vegetation on flow routing and sedimentation patterns: three-dimensional modeling for a tidal marsh. J. Geophys. Res.: Earth Surf. 110 (4), 1–18. https://doi.org/10.1029/2005JF000301.

Temmerman, S., Horstman, E.M., Krauss, K.W., Mullarney, J.C., Pelckmans, I., Schoutens, K., 2023. Marshes and mangroves as nature-based coastal storm buffers. Ann. Rev. Mar. Sci 15, 95–118. https://doi.org/10.1146/annurev-marine-040422-092951.

Temmerman, S., Meire, P., Bouma, T.J., Herman, P.M.J., Ysebaert, T., De Vriend, H.J., 2013. Ecosystem-based coastal defence in the face of global change. Nature 504 (7478), 79–83. https://doi.org/10.1038/nature12859.

Tempest, J.A., Möller, I., Spencer, T., 2015. A review of plant-flow interactions on salt marshes: the importance of vegetation structure and plant mechanical characteristics. Wiley Interdisciplinary Reviews: Water 2 (6), 669–681. https://doi.org/10.1002/WAT2.1103.

Tiessen, M., Vroom, J., van der Werf, J., 2016. Ontwikkeling van het Delft3D FM NeVla model voor het Schelde estuarium - Waterbeweging in de Westerschelde en stroming over de plaat van Walsoorden. Deltares Report, 1220095-000-ZKS-0023, In Dutch.

Van der Spek, A.J.F., 1997. Tidal asymmetry and long-term evolution of Holocene tidal basins in The Netherlands: simulation of palaeo-tides in the Schelde estuary. Mar. Geol. 141 (1–4), 71–90. https://doi.org/10.1016/S0025-3227(97)00064-9.

Van der Wal, D., Wielemaker-Van den Dool, A., Herman, P.M.J., 2008. Spatial patterns, rates and mechanisms of saltmarsh cycles (Westerschelde, The Netherlands). Estuar. Coast Shelf Sci. 76 (2), 357–368. https://doi.org/10.1016/j.ecss.2007.07.017.

van Veelen, T.J., Fairchild, T.P., Reeve, D.E., Karunarathna, H., 2020. Experimental study on vegetation flexibility as control parameter for wave damping and velocity structure. Coast. Eng. 157 (February 2019). https://doi.org/10.1016/j.coastaleng.2020.103648.

van Zelst, V.T.M., Dijkstra, J.T., van Wesenbeeck, B.K., Eilander, D., Morris, E.P., Winsemius, H.C., Ward, P.J., de Vries, M.B., 2021. Cutting the costs of coastal protection by integrating vegetation in flood defences. Nat. Commun. 12 (1), 1–11. https://doi.org/10.1038/s41467-021-26887-4.

Vuik, V., Jonkman, S.N., Borsje, B.W., Suzuki, T., 2016. Nature-based flood protection: the efficiency of vegetated foreshores for reducing wave loads on coastal dikes. Coast. Eng. 116, 42–56. https://doi.org/10.1016/j.coastaleng.2016.06.001.

Vuik, V., Suh Heo, H.Y., Zhu, Z., Borsje, B.W., Jonkman, S.N., 2018. Stem breakage of salt marsh vegetation under wave forcing: a field and model study. Estuar. Coast Shelf Sci. 200, 41–58. https://doi.org/10.1016/j.ecss.2017.09.028.

Wang, H., van der Wal, D., Li, X., van Belzen, J., Herman, P.M.J., Hu, Z., Ge, Z., Zhang, L., Bouma, T.J., 2017. Zooming in and out: scale dependence of extrinsic and intrinsic factors affecting salt marsh erosion. J. Geophys. Res.: Earth Surf. 122 (7), 1455–1470. https://doi.org/10.1002/2016JF004193.

Weisscher, S.A.H., Baar, A.W., van Belzen, J., Bouma, T.J., Kleinhans, M.G., 2022. Transitional polders along estuaries: driving land-level rise and reducing flood propagation. Nature-Based Solutions 2 (June), 100022. https://doi.org/10.1016/j.nbsj.2022.100022.

Willemsen, P.W.J.M., Borsje, B.W., Vuik, V., Bouma, T.J., Hulscher, S.J.M.H., 2020. Field-based decadal wave attenuating capacity of combined tidal flats and salt marshes. Coast. Eng. 156 (January), 103628. https://doi.org/10.1016/j.coastaleng.2019.103628.

Willemsen, P.W.J.M., Smits, B.P., Borsje, B.W., Herman, P.M.J., Dijkstra, J.T., Bouma, T.J., Hulscher, S.J.M.H., 2022. Modeling decadal salt marsh development: variability of the salt marsh edge under influence of waves and sediment availability. Water Resour. Res. 58 (1), 1–23. https://doi.org/10.1029/2020WR028962.

Ysebaert, T., Yang, S.L., Zhang, L., He, Q., Bouma, T.J., Herman, P.M.J., 2011. Wave attenuation by two contrasting ecosystem engineering salt marsh macrophytes in the intertidal pioneer zone. Wetlands 31 (6), 1043–1054. https://doi.org/10.1007/s13157-011-0240-1.

Zhu, Z., Yang, Z., Bouma, T.J., 2020. Biomechanical properties of marsh vegetation in space and time: effects of salinity, inundation and seasonality. Ann. Bot. 125 (2), 277–289. https://doi.org/10.1093/aob/mcz063.

Zijl, F., Sumihar, J., Verlaan, M., 2015. Application of data assimilation for improved operational water level forecasting on the northwest European shelf and North Sea. Ocean Dynamics 65 (12), 1699–1716. https://doi.org/10.1007/s10236-015-0898-7.

Zijl, F., Verlaan, M., Gerritsen, H., 2013. Improved water-level forecasting for the northwest European shelf and North Sea through direct modelling of tide, surge and non-linear interaction topical collection on the 16th biennial workshop of the joint numerical sea modelling group (JONSMOD) in bre. Ocean Dynamics 63 (7), 823–847. https://doi.org/10.1007/s10236-013-0624-2.